# Spray Formation by Turbulent Jets

Because of the desirability in many technological contexts of nozzles that produce jets that are fully turbulent from the start, there has been extensive testing of many nozzle designed with this objective in mind. Simmons (1977) makes the useful observation that sprays produced by a wide range of nozzle designs have similar droplet size distributions when these are compared in a *root/normal* graph as shown in figure 1. Here the ordinate corresponds to $(D/D_m)^{\frac{1}{2}}$ where $D_m$ is the mass mean diameter (see section (Nad)). The horizontal scale is stretched to correspond to a normal distribution. The straight line to which all the data collapse implies that $(D/D_m)^{\frac{1}{2}}$ follows a normal distribution. Since the size distributions from many different nozzles all have the same form, this implies that the sprays from all these nozzles can be characterized by a single diameter, $D_m$. An alternative measure is the Sauter mean diameter, $D_s$, since $D_s/D_m$ will have the universal value of 1.2 under these circumstances.

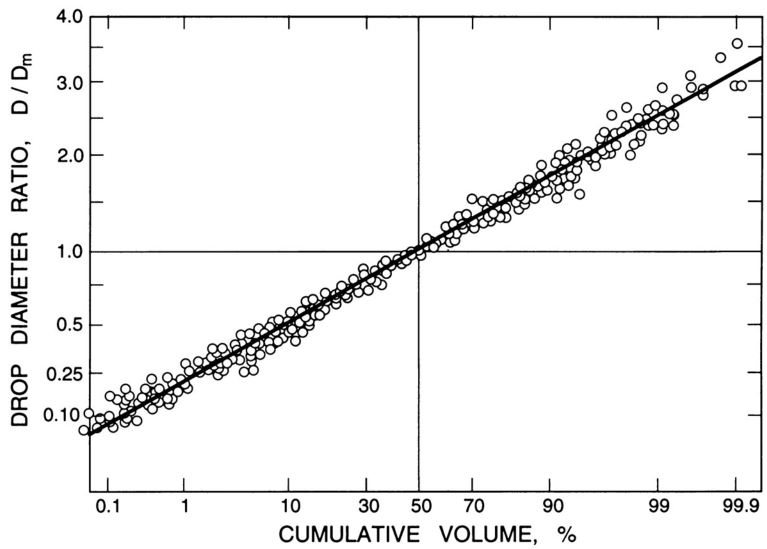


Figure 1: The distribution of droplet sizes in sprays from many types of nozzles plotted on a root/normal graph. Adapted from Simmons (1977).

Early studies of liquid jets by Lee and Spencer (1933) and others revealed that the turbulence in a liquid jet was the primary initiator of break-up. Subsequent studies (for example, Phinney 1973, Hoyt and Taylor 1977a,b, Ervine and Falvey 1987, Wu *et al.* 1995, Sarpkaya and Merrill 1998) have examined how this process works. In the early stages of breakup, the turbulent structures in the jet produce ligaments that project into the gaseous phase and then fragment to form droplets as illustrated in figure 1, section Noe). The studies by Wu *et al.* (1995) and others indicate that the very smallest structures in the turbulence do not have the energy to overcome the restraining forces of surface tension. However, since the smaller turbulent structures distort the free surface more rapidly than the larger structures, the first ligaments and droplets to appear are generated by the smallest scale structures that *are* able to overcome surface tension. This produces small droplets. But these small structures also decay more rapidly with distance from the nozzle. Consequently, further downstream progressively larger structures cause larger ligaments and droplets and therefore add droplets at the higher end of the size distribution. Finally, the largest turbulent structures comparable with the jet diameter or width initiate the final stage of jet decomposition as illustrated in figure 2.

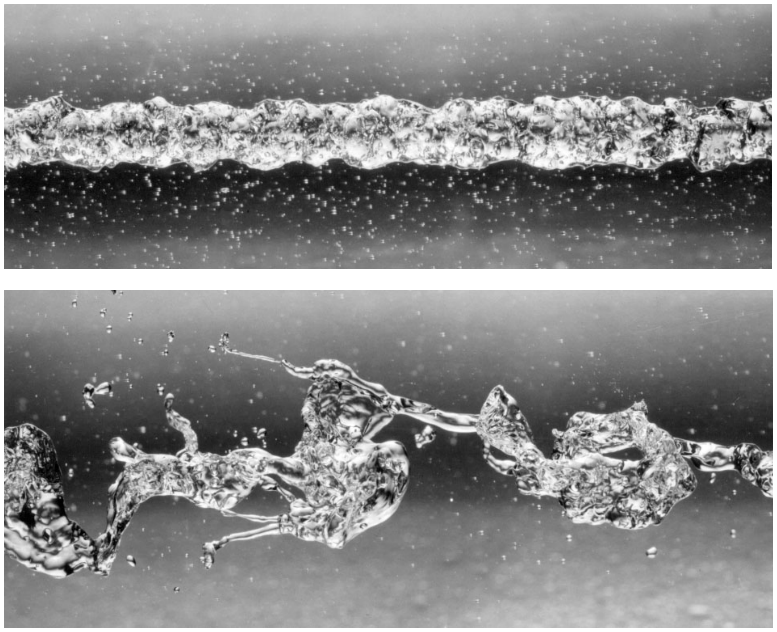

Figure 2: A continuation from figure 1, section (Noe), showing two further views of the jet at 72 diameters (above) and 312 diameters (below) downstream from the nozzle. The latter illustrates the final breakup of the jet. Reproduced from Hoyt and Taylor (1977b) with the permission of the authors.

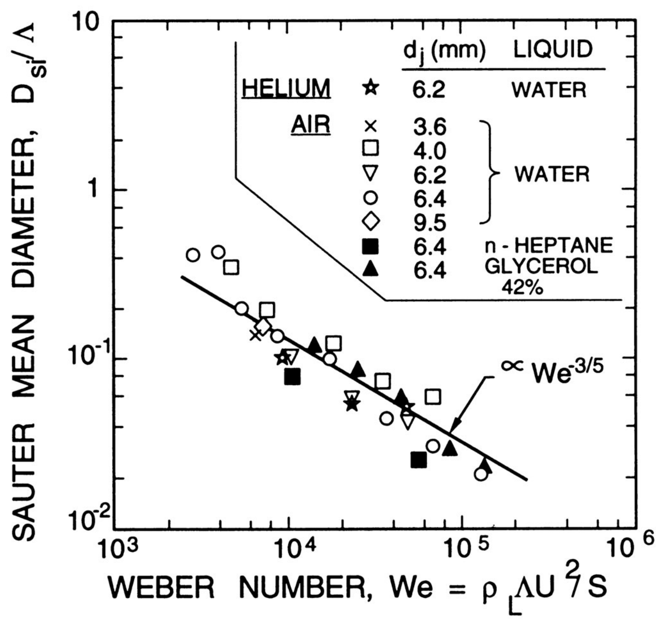


Figure 3: The Sauter mean diameter, $D_{si}$, of the initial droplets formed (divided by the typical dimension of the jet, $\Lambda$) in turbulent round jets as a function of the Weber number, $We = \rho_L \Lambda U^2/S$. The points are experimental measurements for various liquids and jet diameters, $d_j$. Adapted from Wu *et al.* (1995).

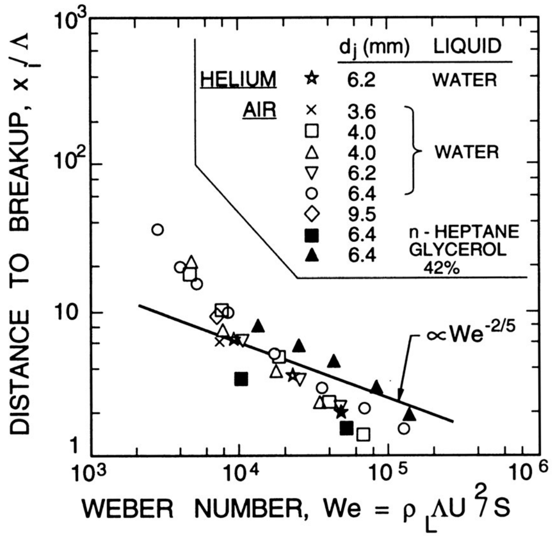


Figure 4: The ratio of the distance from the nozzle to the point where turbulent breakup begins (divided by $\Lambda$) for turbulent round jets as a function of the Weber number, $We = \rho_L \Lambda U^2/S$. The points are experimental measurements for various liquids and jet diameters, $d_j$. Adapted from Wu *et al.* (1995).

Wu, Miranda and Faeth (1995) utilized this understanding of the spray formation and jet breakup process to create scaling laws of the phenomenon. With a view to generalizing the results to turbulent jets of other cross-sections, the radial integral length scale of the turbulence is denoted by $4\Lambda$ where, in the case of round jets, $\Lambda = d_j/8$, where $d_j$ is the jet diameter. Wu *et al.* (1995) then argue that the critical condition for the initial formation of a droplet (the so-called primary breakup condition) occurs when the kinetic energy of a turbulent eddy of the critical size is equal to the surface energy required to form a droplet of that size. This leads to the following expression for the Sauter mean diameter of the initial droplets, $D_{si}$:

$$\frac{D_{si}}{\Lambda} \propto We^{-\frac{3}{5}} \tag{Nof1}$$

where the Weber number, $We = \rho_L \Lambda U^2$, $U$ being the typical or mean velocity of the jet. Figure 3 from Wu *et al.* (1995) demonstrates that data from a range of experiments with round jets confirm that $D_{si}/\Lambda$ does appear to be a function only of $We$ and that the correlation is close to the form given in equation (Nof1).

Wu *et al.* (1995) further argue that the distance, $x_i$, from the nozzle to the place where primary droplet formation takes place may be estimated using an eddy convection velocity equal to $U$ and the time required for Rayleigh breakup of a ligament having a diameter equal to the $D_{si}$. This leads to

$$\frac{x_i}{\Lambda} \propto We^{-\frac{2}{5}} \tag{Nof2}$$

and, as shown in figure 4, the data for different liquids and jet diameters are in rough accord with this correlation.

Downstream of the point where primary droplet formation occurs, progressively larger eddies produce larger droplets and Wu *et al.* (1995) use extensions of their theory to generate the following expression for the Sauter mean diameter, $D_s$, of the droplets formed at a distance, $x$, downstream of the nozzle:

$$\frac{D_s}{\Lambda} \propto \left( \frac{x}{\Lambda We^{\frac{1}{2}}} \right)^{\frac{2}{3}} \tag{Nof3}$$

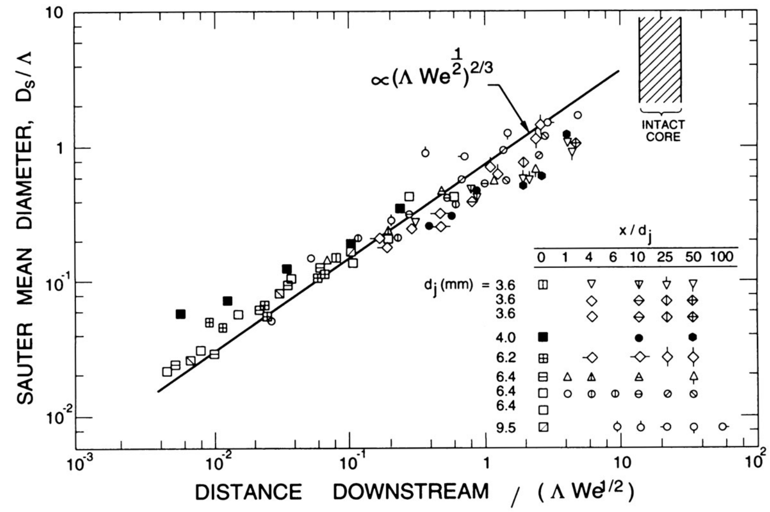


Figure 5: The Sauter mean diameter, $D_s$ (divided by $\Lambda$), of the droplets formed at a distance, $x$, from the nozzle for turbulent round jets for various Weber numbers, $We = \rho_L \Lambda U^2/S$. The points are experimental measurements for various liquids and jet diameters, $d_j$. Adapted from Wu *et al.* (1995).

As shown in figure 5 the experimental measurements show fair agreement with this approximate theory.

Using this information, the evolution of the droplet size distribution with distance from the nozzle can be constructed as follows. Assuming Simmons size distributions, the droplet size distribution may be characterized by the Sauter mean diameter, $D_s$. The primary breakup yields droplets characterized by the initial $D_{si}$ of equation (Nof1). Then, moving downstream along the jet, contributions with progressively larger droplets are added until the jet finally disintegrates completely.

Several footnotes should be added to this picture. First, the evolution described assumes that the gaseous phase plays a negligible role in the dynamics. Wu and Faeth (1993) demonstrate that this will only be the case when $\rho_L/\rho_G > 500$. However this is frequently the case in practical applications. Second, the above can be extended to other free jet geometries. Dai *et al.* (1998) demonstrate that the simple use of a hydraulic diameter allows the same correlations to be used for plane jets. On the other hand, wall jets appear to follow different correlations presumably because the generation of vorticity in wall jets causes a different evolution of the turbulence than occurs in free jets (Dai *et al.* 1997, Sarpkaya and Merrill 1998). Sarpkaya and Merrill's (1998) experiments with wall jets on horizontal smooth and roughened walls exhibit a ligament formation process qualitatively similar to that of free jets. The droplets created by the ligament breakup have a diameter about 0.6 of the wall jet thickness and quite independent of Weber number or plate roughness over the range tested.

Finally, the reader will note that the above characterizations are notably incomplete since they do not address the issue of the total number or mass of droplets produced at each stage in the process. Though this is crucial information in many technological contexts, it has yet to be satisfactorily modeled.